Silica-Free Mullite Structures in the Al$_2$O$_3$–B$_2$O$_3$–P$_2$O$_5$ Ternary System

D. Mazza,* S. Ronchetti, and A. Delmastro

*Dipartimento di Scienza dei Materiali ed Ingegneria Chimica,
Politecnico di Torino, Torino, Italy*

M. Tribaudino

Dipartimento di Scienze Mineralogiche, Università di Torino, Torino, Italy

W. Kockelmann

Rutherford Appleton Laboratories, Cambridge, U.K.

Received May 25, 2000. Revised Manuscript Received September 22, 2000

The stability of silica-free mullite structures in the Al$_2$O$_3$–B$_2$O$_3$–P$_2$O$_5$ ternary system was investigated at $T = 900$–1000 °C. A monophasic mullite was obtained for the composition Al$_8$BPO$_{16}$, showing that substitution of P and B for Si is possible for 2:1 mullite, Al$_4$SiO$_8$, while the same substitution for the 3:2 mullite yielded a biphasic mixture. Another monophasic sample was obtained in the same temperature range, with composition Al$_{8.6}$P$_{0.4}$B$_{1.6}$O$_{16.3}$. Further preparations close to the above compositions enabled us to assess the homogeneity range for these silica-free mullites. At 1000 °C it can be expressed by the following notation: Al$_{8+x}$P$_{1-x}$B$_{1+x}$O$_{16+x/2}$ with $0 \leq x \leq 0.6 \pm 0.1$. The stability range expressed by the above relation results lie on the join 2:1 silica-free mullite–Al$_9$B$_2$O$_{16.5}$. Neutron and X-ray powder diffraction were performed on the two limit compositions (with $x = 0$ and $x = 0.6$), showing that phosporus is likely to enter the tetrahedral T site. Boron occupies a site with triangular coordination, between T and T* sites, at a distance of 0.6 Å from the center of the T polyhedron.

Introduction

Mullite is one of the most investigated ceramic compounds, for its refractory properties and specific structural nature. Mullite has a general notation [Al$_2$]Al$_{2+2x}$Si$_{2-2x}$O$_{10-x}$□$_x$. (Hereinafter brackets indicate octhedral sites, no brackets indicate tetrahedral sites, and □ stands for a vacancy.) The limit values for the x parameter, according to a recent optimization of the SiO$_2$–Al$_2$O$_3$ phase diagram,[1] vary with temperature, but they are comprised between $x = 0.4$ (2:1 mullite) and $x = 0.25$ (3:2 mullite). Over this general formula large chemical substitution may occur.

The incorporation of ions different from Al and Si into the mullite structure has been examined from the point of view of structural chemistry, mineralizing action in the synthesis, and special properties of the substituted mullite. Up to a certain degree, Cr, Ti, V, Mn, Fe, and trivalent Co can relatively easily enter the octahedral sites of the structure and substitute for Al^{3+},[2–4] while other transition metal ions, in their divalent oxidation state, like Ni, Co, and Cu, only promote the formation of unsubstituted mullite, forming contemporarily a finely divided spinel phase.[5] Alkaline metal ions such as Na$^+$ or K$^+$ can also stabilize a silica-free mullite structure by insertion in sites with 8-fold coordination. The phase stability is however limited to 800–1000 °C.[6]

The substitution of Si or Al on the tetrahedral sites[7] of the mullite structure might be in principle possible with similar ionic size atoms, such as B^{3+}, P^{5+}, and Al^{3+}. Boron alone can stabilize silica-free metastable mullite structures[6] with a composition comprised between A$_5$BO$_9$ and A$_4$B$_2$O$_9$. In these structures boron displays 3-fold as well as 4-fold coordination.

The aliovalent P substitution for Si/Al on the tetrahedral sites seems not viable, as no mullitic phases are found in the pseudobinary system AlPO$_4$–SiO$_2$.[8] In principle, the coupled isovalent substitution of (B + P) for 2 Si should be considered; however in the Al$_2$O$_3$–B$_2$O$_3$–P$_2$O$_5$ system as reviewed in the past by Hummel and Horn[9,10] no such phases were found. This system

* Corresponding author: Tel.: +39-11-5644688. Fax: +39-11-5644699. E-mail: mazza@polito.it.

(1) Eriksson, G.; Pelton, A. D. *Metall. Trans.* **1993**, *24B*, 807.
(2) Murthy, M. K.; Hummel, F. A. *J. Am. Ceram. Soc.* **1960**, *43* (5), 267.
(3) Rager, H.; Schneider, H.; Graetsch, H. *Am. Mineral.* **1990**, *75*, 392.
(4) Chadhuri, S. P.; Patra, S. K. *Br. Ceram. Trans.* **1997**, *96* (3), 105.
(5) Mazza, D.; Delmastro, A.; Ronchetti, S. *J. Europ. Ceram. Soc.* **2000**, *20*, 699.
(6) Mazza, D.; Vallino, M.; Busca, G. *J. Am. Ceram. Soc.* **1992**, *75* (7), 1929.
(7) Angel, R. J.; Prewitt, C. T. *Am. Mineral.* **1986**, *71*, 1476.
(8) Takahashi, T.; Agrawal, D. K.; Roy, R. *Structural Control of Phase Formation in Low-Temperature AlPO$_4$–SiO$_2$ Reactions.*
(9) Horn, W. F.; Hummel, F. A. *Trans. J. Br. Ceram. Soc.* **1980**, *79*, 109.
(10) Hummel, F. A.; Horn, W. F. *J. Aust. Ceram. Soc.* **1981**, *17*, 1.

Table 1. Phases Revealed by Powder XRD after Crystallization and Shape of the Crystallization Peaks

sample	composn	cryst temp (°C)	phase(s) at 1000 °C for 20 min heating time	crystallization peak by DTA/TG.
A ($x = 0.5$)	$Al_{10}BPO_{19}$	1000	mullite-like phase + tridymite + γ-allumina	broad with no weight loss
B ($x = 0.45$)	$Al_9BPO_{17.5}$	1000	mullite-like phase + tridymite + γ-allumina	broad with no weight loss
C ($x = 0.4$)	Al_8BPO_{16}	980	pure mullite-like phase	sharp with 2 wt % loss 50 °C before and during crystallization, peak asymmetric
D ($x = 0.25$)	Al_6BPO_{13}	980	mullite-like phase + tridymite	sharp with 2 wt % loss 50 °C before and during crystallization
E ($x = 0$)	Al_4BPO_{10}	940	Al_9B_2 + high-crystobalite s.s. term	less sharp with 2 wt % loss during crystallization
F (x does not apply)	Al_2BPO_7	850	Al_2B + high-crystobalite s.s. term	less sharp with 1.5 wt % loss during crystallization
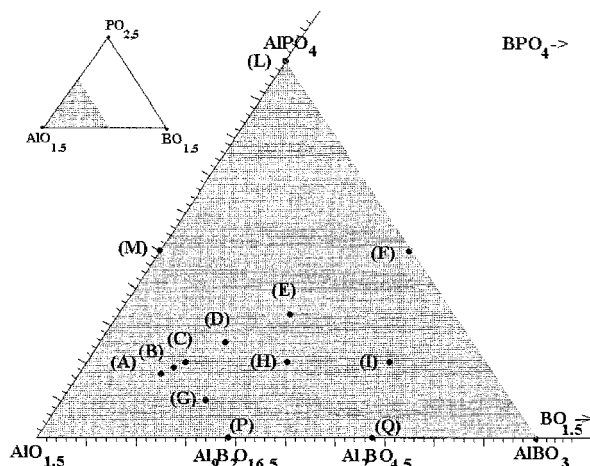
Figure 1. The ternary system and the explored compositions (atomic ratio).

was however studied by conventional solid-state reactions between alumina, boric acid, and ammonium diacid phosphate to prepare samples by reaction at 1215 °C in air with heavy losses in both B_2O_3 and in P_2O_5 by sublimation, which required further chemical analyses to check the final compositions. At the above temperature no ternary phases were revealed; the only binary crystalline phases revealed by X-ray diffraction were $Al_9B_2O_{16.5}$ and a solid solution series between $AlPO_4$ and BPO_4 having high (β) crystobalite structure.

To assess the stability of ternary mullite-like phases we reexamined the same ternary system at lower (900–1000 °C) temperatures by employing wet chemical synthesis. This route comprises the formation of amorphous precursors at low temperature (500 °C), followed by their crystallization, at a significantly lower temperature with respect to ceramic route, thus avoiding B_2O_3 or P_2O_5 sublimation.[11,12] The aim of this research was to verify the possibility of the substitution of (B + P) for 2 Si atoms in the 3:2 and 2:1 mullite structures. The mullites substituted according to our hypothesis should correspond to the notation $[Al_2]Al_{2+2x}P_{1-x}B_{1-x}O_{10-x}\square_x$. To confirm the above hypothesis we first investigated the compositions A–F of Figure 1 and Table 1, which correspond to different x values in the above formula. Thereafter, other compositions were prepared and XRD-analyzed, to assess the homogeneity range and the phase relationships in the alumina-rich part of the ternary phase diagram.

In the concluding section the results of structural refinement on X-ray and neutron powder diffraction data for two mullites synthesized in this work are reported, to determine the site partitioning of the P and B cations.

Experimental Section

Synthesis of the Precursors. The mullite reactive precursors were obtained by the wet chemical route. Starting materials were $Al(NO_3)_3 \cdot 9H_2O$ (Fluka 99.9% purity), boric acid (Carlo Erba), and ammonium diacid phosphate. Mixtures of appropriate ratios were placed in porcelain dish and 10 wt % of reducing agent (glycerol) was added together with small amounts of distilled water. Glycerol reacts with boric acid even at room temperature to form ester complexes, therefore preventing volatilization of boric acid at temperatures higher than 100 °C and increasing contemporarily the otherwise low solubility of the boric acid in water.

The components dissolved below 100 °C, forming a single liquid phase which was further heated at 150 °C, when aluminum nitrate begins to decompose with a redox reaction, emitting brown colored gases (NO_x, CO, CO_2, and H_2O). After completion of the reaction, the obtained spongy, bulky solid was then transferred into at 400 °C and then 500 °C oven for 30 min in order to completely remove nitrogen oxides and to oxidize the remaining organic matter.

The resulting xerogels were amorphous when examined by X-ray diffraction. In these materials the degree of mixing between the component oxides is extimated to be on the nanometer scale, as indicated by the low crystallization temperatures[13] and by the dimensions of the crystal grains after crystallization (100–150 nm) as shown in Figure 2a by a HR-TEM image of sample C after crystallization at 1000 °C. Moreover the xerogels were examined by simultaneous DTA/TG in air in order to assess the crystallization temperature indicated by the exothermic peak and to verify any weigh loss occurred at high temperature, given previous issues with P, B volatility ($10°$/min heating rate up to 1300 °C, open container in flowing chromatographic air 2 L/min, ≈50 mg each test). Figure 3 reports one of these curves (sample C) exhibiting the weight loss of the amorphous mass between 400 and 800 °C and the exotherm peak of crystallization about 980 °C. After crystallization and up to 1300 °C no weight loss appears in TG patterns thus ensuring compositional stoichiometry.

Heat Treatments on the Precursors. Different batches of precursor, ground in an agate planetary mixer and then isostatically cold pressed in pellets (10 GPa), were heated at the crystallization temperature, indicated by DTA exotherm, for 1 h in air. The phases formed at this temperature were checked by XRD. Thereafter the materials were heated in air at 1000 °C for 20 min, to study the phase relationships at this temperature avoiding ambiguity due to different crystallization temperatures. The results are listed in Table 1. Finally the samples were heated to 1300 °C for 5 min (in these last conditions the weight loss is confined to 0.2–0.6 wt %, as

(11) Abbattista, F.; Delmastro, A.; Gozzelino, G.; Mazza, D.; Vallino, M.; Busca, G.; Lorenzelli, V. *J. Chem. Soc., Faraday Trans.* **1990**, *86* (21), 3653.

(12) Delmastro, A.; Gozzelino, G.; Mazza, D.; Vallino, M.; Busca, G.; Lorenzelli, V. *J. Chem. Soc., Faraday Trans.* **1992**, *88* (14), 2065.

(13) Aksay, I. A.; Tabbs, D. M. and Sarikaya, M. *J. Am. Ceram. Soc.* **1991**, *74* (10), 2343.
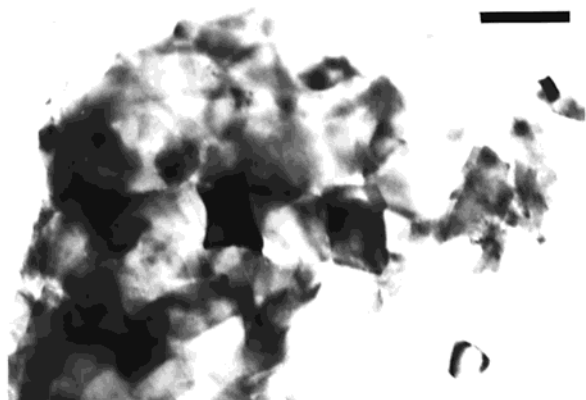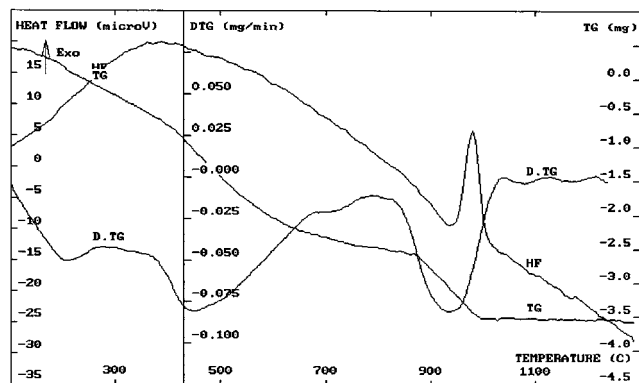
Figure 2. (a) TEM bright-field imaging of the G sample. Scale bar = 1500 Å. (b) Selected area diffraction pattern taken on the same area as (a). Note the polycrystalline pattern.

Figure 3. Differential thermal analysis (HF) and thermogravimetric profile (TG).

evidenced by TGA), to test the temperature stability of the phases evidenced at 1000 °C. The obtained samples were also examined with a CM12 transmission electron microscope, operated at 120 kV. The samples turned out to be an aggregate of crystals sized about 0.1 μm (Figure 2).

Structural Refinement. Neutron diffraction was performed on the two monophasic compositions at 1000 °C (C and G; see subsequent discussion), to verify their structure. The assessment of the site occupancies was performed by both neutron and X-ray diffraction, exploiting the different scattering characteristics of the different elements. For neutron diffraction the compositions C and G were synthesized using B[11]-enriched (99%) boric acid, to avoid the strong absorption of B-10. X-ray diffraction was carried out on a Philips X'Pert

Table 2. Phases Revealed by Powder XRD after Crystallization at 1000 °C

sample	composn	cryst temp (°C)	phase(s) at 1000 °C for 20 min heating time
G	$Al_{16.2}B_{2.8}PO_{31}$	980	pure mullite-like phase
H	$Al_7B_2PO_{16}$	910	Al_9B_2 + high-crystobalite s.s. term
I	$Al_6B_3PO_{16}$	830	Al_2B + high-crystobalite s.s. term
L	$AlPO_4$		
M	Al_3PO_7	600	γ-alumina + tridymite
P	$Al_9B_2O_{16.5}$	855	Al_9B_2 (no. 320003)
Q	$Al_2BO_{4.5}$		Al_2B (no. 290010, Uhlig et al.)

powder diffractometer using a Cu Kα radiation and a graphite monochromator. The spectra were taken with 2θ between 25 and 95°. Neutron diffraction was performed on the ROTAX powder diffractometer at the ISIS spallation source at the Rutherford Appleton Laboratory, Cambridge, United Kingdom. Three banks were used to collect the data at $2\theta = 25.2$, 65.3, and 122.4°, respectively, accessing d spacings down to 0.3 Å. Neutron and X-ray data were processed separately using the GSAS refinement package of powder spectra.[14] In a first stage the atomic coordinates were not refined and peak profiles, cell parameters, and backgrounds were refined with a LeBail procedure;[15] after satisfactory profile fitting the coordinates were released. The P and B atoms were assigned by both X-ray and neutron refinement in several models to verify their structural position.

A refinement of the displacement parameters was done at the end of data processing, by constraining the parameters of Oab and Od and Oc and Oc*, as well as Al, T, T*, and B sites, respectively, to have the same isotropic parameter (these symbols refer to crystallographic positions of mullite, as in Table 4). The obtained displacement parameters were assigned to the X-ray input. At this stage a site refinement of the total scattering factor of sites T and T* was carried out using the only constraint that P resides fully on the T site. Oc and Oc* occupancies were refined by neutron diffraction data and used in the X-ray refinements. The obtained structural parameters and site occupancies are shown in Tables 3−5. At the end of the refinement cycles for sample C the neutron data refinements yielded R_p = 4.2, 4.0, and 4.4% and $R(F2)$ = 4.1, 8.3, and 9.9% for the spectra collected with the three neutron detector banks. The corresponding values for sample G are R_p = 3.5, 3.6, and 2.9% and $R(F2)$ = 2.2, 6.7, and 6.4%.

Results and Discussion

Stability of P- and B-Substituted Mullites. Table 1 shows the compositions of the samples A−F along the diagonal of the phase diagram, the "*x*" value in the general formula $[Al_2]Al_{2+2x}P_{1-x}B_{1-x}O_{10-x}\square_x$, the crystallization temperature, the phases present at 1000 °C, and the crystallization peak by DTA/TG. No difference was noticed in phase compositions between 1000 °C and the crystallization temperature. On the contrary, the samples up to 1300 °C exhibited enhanced phase transformation, as discussed below.

The composition Al_8BPO_{16} (sample C, $x = 0.4$) was found to be monophasic after crystallization at 1000 °C. This composition derives formally from the 2:1 mullite composition (Al_4SiO_8), where silicon is replaced by half boron plus half phosphorus, thus confirming the above substitutional hypothesis only for 2:1 mullite. The other samples, however, having higher or lower *x* values are bi- or triphasic. In the XRD measurements sample D,

(14) Larson, C.; Von Dreele, R. B. GSAS General Software Analysis manual, Los Alamos National Laboratory report, LA-UR 86-87.

(15) LeBail, A.; Duroy, H.; Fourquet, J. L. *Mater. Res. Bull.* **1988**, *23*, 447.

Table 3. Neutron Atomic Fractional Coordinates, Isotropic Displacement Factors (10⁻² Å), and Predicted−Observed Site Occupancies (Fraction on Total Occupancy) for Sample C

	frac occ	x	y	z	U_{iso}	predicted	X-ray	neutron
Al (2a)	1.0	0	0	0	1.7(1)	1.0	1.0	0
T (4h)	0.51(1) Al	0.160(1)	0.3397(8)	0.5	1.7(1)	0.50 Al	0.46(1)	0.51(1)
	0.15 P	0.160(1)	0.3397(8)			0.15 P	0.15	0.15
T* (4h)	0.19(1) Al	0.273(3)	0.199(3)	0.5	1.7(1)	0.20 Al	0.24(1)	0.19(1)
B (4h)	0.15	0.215(4)	0.286(4)	0.5	1.7(1)	0.15	0.15	0.15
Oab (4g)	1.0	0.3613(4)	0.4188(3)	0.5	2.4(1)	1.0	1.0	1.0
Oc (2d)	0.40	0.5	0	0.5	2.4(1)	0.40	0.40	0.40
Oc* (4h)	0.20	0.455(2)	0.053(2)	0.5	2.4(1)	0.20	0.20	0.20
Od (4h)	1.0	0.1318(5)	0.2144(3)	0	2.4(1)	1.0	1.0	1.0

Table 4. Interatomic Distances from Neutron Diffraction Experiments, and the Literature (for 2:1 Mullite)

dists (Å)	sample C neutron	sample G neutron	2:1 mullite[7]
Al−Oab ×4	1.876(2)	1.879(1)	1.8936(5)
Al−Od ×2	1.926(3)	1.929(1)	1.9366(9)
av	1.901	1.904	1.908
T−Oab	1.64(1)	1.714(5)	1.7102(8)
T−Oc	1.727(7)	1.678(4)	1.6676(2)
T−Od ×2	1.731(4)	1.716(2)	1.7273(5)
av	1.699	1.706	1.708
T*−Oab	1.82(3)	1.86(1)	1.8166(11)
T*−Oc*	1.778(2) (§)	1.76(2)[a]	1.8522(4)
T*−Od ×2	1.79(1)	1.746(1)	1.7727(7)
av	1.796	1.78	1.803
B−Oab	1.50(3)	1.49(1)	
B−Od ×2	1.65(1)	1.641(6)	
av	1.575	1.59	

[a] This distance was soft constrained to 1.78 Å during the last refinements cycles.
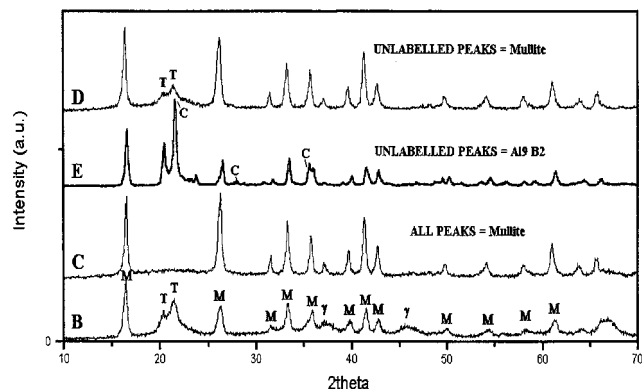
Figure 4. X-ray powder patterns for B−E compositions heat treated at 1000 °C (T = AlPO₄-tridymite, C = high (β) cristobalite solid solution, M = silica-free mullite, γ = γ-alumina; same symbols apply to Figures 5 and 6).

which formally derives from 3:2 mullite ($Al_6Si_2O_{13}$) by silicon replacement, displays tridymite-like $AlPO_4$ and the mullite-type peaks of sample C with the same lattice parameters. Also sample E (Al_4BPO_{10}), which formally derives from andalusite (or sillimanite) Al_2SiO_5 by silicon replacement, resulted as biphasic (see Figure 4). These results suggest that vacancies have a stabilizing effect on the structure. This would appear unusual for such a defective structure, unless some kind of long-range order periodicity is present, like it occurs with incommensurate periodicity in the Si bearing mullite. The lack of crystals large enough for TEM observation made it impossible to verify the presence of such an incommensurate periodicity which is herefore only speculative at present. The crystallization occours through a diffusion controlled decomposition of the precursors, which leads directly to a mullite-like phase

at temperatures <1000 °C, without formation of $γ-Al_2O_3$, as it is the case for the ($3Al_2O_3$−SiO_2) mullite obtained from noncrystalline precursors.[16]

Samples having $x > 0.4$ gave XRD evidence of γ-alumina and $AlPO_4$-tridymite. It has to be noted that the crystallite size of γ-alumina in these samples falls in the nanometer scale range, as estimated by the peak broadening. This explains perhaps why for these samples the exothermic DTA peaks are much broadened as indicated in Table 1; this table also indicates DTA/TG evidence for the compositions A−F.

After the assessment of a new silica-free mullite phase with the composition C at 980−1000 °C, our further effort was aimed to determine the homogeneity range for this phase and its temperature stability. Other compositions were prepared, and the results of the XRD phase analyses on the samples crystallized at 1000 °C are listed in Table 2. All the compositions were prepared as described above and the xerogels were heated at 1000 °C for 20 min in order to compare the phase stability; it has to be noted however that each one of the new compositions has a lower crystallization temperature. In particular L and M crystallize at very low temperatures (400−500 °C). As a result the 500 °C preparations are already crystalline rather than amorphous. The reason for this can be found in the low-temperature formation of $AlPO_4$-tridymite from corresponding xerogels, as shown by XRD patterns of sample L (not shown). This phase remains stable at 1000 °C, even for prolonged annealing. Above this temperature it transforms to thermodinamically stable high-cristobalite, as pointed out by[10] and confirmed by our findings (see below).

Only sample G results in monophasic with silica-free mullite structure having slightly different lattice parameters compared to sample C. From the examination of the compositions of samples C and G, this phase would have an homogeneity range at 1000 °C which can be tentatively expressed by the relation

$$Al_{8+x}P_{1-x}B_{1+x}O_{16+x/2}$$
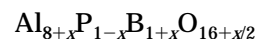
with x varying in the range $0 \leq x \leq 0.6 \pm 0.1$. The stability range expressed by the above relation results lies on the join 2:1 silica-free mullite−Al_9B_2.

A certain small amount of coexisting amorphous phase cannot be excluded at this temperature, which could in principle slightly alter the elemental ratios. The above compositional range and the P presence in the crystal structure even at the $x = 0.6$ value is however confirmed by bond length results as referred to below.

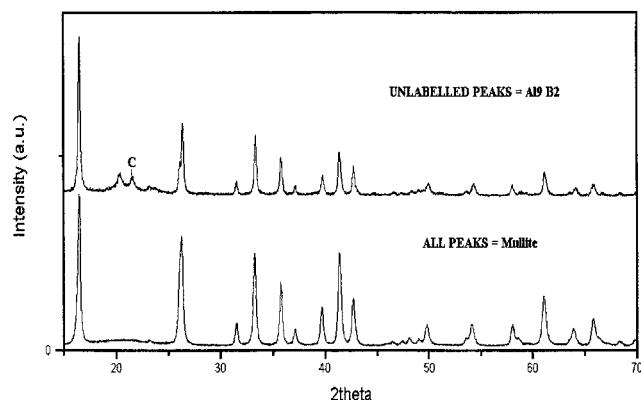(16) Schneider, H.; Merwin, L.; Sebald, A. *J. Mater. Sci.* **1992**, *27*, 805.
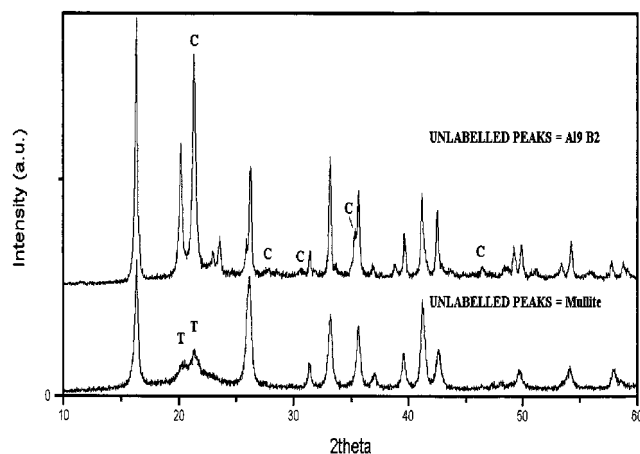
**Figure 5.** X-ray powder patterns for sample C heat treated at 1000 °C (below) and to 1300 °C (above).

The phase evidence obtained on the samples G−Q allows us also to trace the compatibility relationships at 1000 °C in the alumina-rich part of the diagram. At this temperature the mullite-like structures $Al_{6-x}B_xO_9$ are no longer stable,[6] and the two compounds $Al_9B_2O_{16.5}$ and $Al_2BO_{4.5}$ coexist (the latter being stable up to 1035 °C in according to Doerner et al.).[17] It has to be noted that Al_9B_2 and Al_2B and silica-free mullite phase have similar structural features, for example edge-sharing AlO_6 octahedra aligned parallel to *c*. They therefore display unit cell constants which are very similar, in particular $c(Al_9B_2) \approx 2c$(mull), $b(Al_9B_2) \approx 2a$(mull) and $c(Al_2B) \approx 2c$(mull), $a(Al_2B) \approx 2a$(mull), $b(Al_2B) \approx 2b$(mull).

These structural similarities make it difficult to detect the real homogeneity range for the mullite-like phase, particularly for $x > 0.6$, when this phase is in phase equilibrium with Al_9B_2. Therefore the *x*-value of the end term in 0.6 is only tentative. It has to be noted that also a similar solid solution relationship between Al_9B_2 and 3:2 mullite ($Al_6Si_2O_{13}$) was demonstrated by Dietzel and Scholze (from 27.6 to 50% of Al_9B_2).[18] According to evidence from X-ray diffraction Al_9B_2 and Al_4B_2 coexist within a certain range of mixed crystals along the joint $AlPO_4–BPO_4$, with high-cristobalite structure. The composition of the terms of the above range can be calculated from the lattice parameters of the high-cristobalite structure, as indicated by Horn and Hummel.[19] The solid solution series with mullite structure results in equilibrium with γ-Al_2O_3 from one side and with tridymite $AlPO_4$ from the other. The comprehensive ternary phase diagram, based on the above evidence, is shown in Figure 7.

The same ternary system was also examined at 1300 °C in order to check the stability range of $Al_{8+x}P_{1-x}B_{1+x}O_{16+x/2}$. It has to be noted that at this temperature Al_2B composition is no longer stable, in agreement with Doerner et al.[18] The compositions A−C and G do not indicate silica-free mullite. On the contrary XRD shows only Al_9B_2 and a high-cristobalite solid solution (Figures 6 and 7). The XRD evidence on the other composition

(17) Doerner, P.; Gauckler, L. J.; Krieg, H.; Lukas, H. L., Petzow, G.; Weiss, J. *CALPHAD* **1979**, *3*, 241.

(18) Dietzel; Scholze. *Glastech. Ber.* **1955**, *28* (2), 47.

(19) Horn, W. F.; Hummel, F. A. *Trans. J. Br. Ceram. Soc.* **1979**, *78* (4), 158.

Figure 6. X-ray powder patterns for sample G heat treated at 1000 °C (below) and to 1300 °C (above).
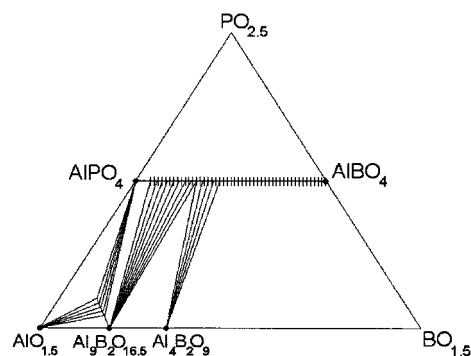
Figure 7. Ternary phase diagram at 1000 °C. (+++ denotes a solid solution.)

heated at 1300 °C confirmed these results, in agreement with the compatibility triangle $Al_2O_3–P_2O_5–B_2O_3$ referred as "probable" by Hummel and Horn[10] at 1200 °C. The only remaining binary composition Al_9B_2 results therefore in equilibrium with the whole series of high-crystobalite s.s. term.

Site Occupancies and B Coordination. X-ray and neutron structural refinements allowed us to clarify the site occupancy in the mullite structure. Site occupancy refinement of mullite-type structures is not straightforward as partial site occupancy is present in these structures dominated by vacancies. The structure of mullite can be derived from that of the mineral sillimanite. In sillimanite tetrahedral sites are ordered and occupied by 0.5 Al and 0.5 Si; the substitution of some Si by Al on tetrahedral sites induces structural disorder on these sites accompanied by simultaneous removal of oxygens according to the scheme $O^{2-} + 2Si^{4+} = 2Al^{3+} + \square$. As a result vacancies are introduced into the structure. This substitution gives rise to the formation of two partially occupied sites (T and T*) in which either Si or Al can be present, owing to the disordered nature of the mullite structure. On the basis of detailed examination of bond lengths and of the oxygens displacement tensors, it was suggested by Angel and Prewitt[7] that Si does not occupy the T* site. In their work however conclusive evidence was hindered by the low reliability of site occupancy refinement of very similar X-ray scatterers such as Al and Si. In the present work Si is substituted by P and B in sample C and by Al, P, and B in sample G. There is a significant neutron scattering contrast between P, B, and Al with scattering lengths of 0.513×10^{-12}, 0.665×10^{-12}, and

0.335×10^{-12}, respectively, but also a higher X-ray scattering contrast in comparison to the contrast between Si and Al. The refinement of the T and T* site occupancy was therefore done with X-ray and neutron data to verify their site partitioning. A theoretical constraint on site occupancies was shown by Angel and Prewitt[7] for 2:1 mullites. Starting from the general formula of mullite $[Al_2]Al_{2+2x}Si_{2-2x}O_{10-x}$, simple considerations show that fractional occupancies are the following: $Oc = 1 - 3x/2$; $Oc^* = x/2$; $Al(T + T^*) = 0.5 + x/2$; $Si(T + T^*) = 0.5 - x/2$. For sample C ($x = 0.4$), where P and B completely substitute for Si, these constraints lead to relation $B + P(T + T^*) = 1$. At first site occupancies were refined in sample C, by fixing the occupancies of oxygens Oc and Oc* to the theoretical values and ascribing all B and P to the T site, in agreement with the suggestions of Angel and Prewitt.[7] Initial anomalous results and poor convergence disappeared with the release of the B coordinates and independent refinement to a site with a distance of 0.6 Å to site T.

The comparison between the neutron-refined site occupancies in the C sample and the expected values are reported in Table 3. By allowance of a phosphorus exchange between T and T*, the quality of the fits does not vary much. Change of P occupancy is compensated by change of Al occupancies on both lacunar 4h positions, so that the P location in the structure can only be inferred indirectly, as follows. X-ray and neutron refinements show that, assuming that Al is the only atom in the T* site, i.e., B and P do not enter that site, the refined Al content almost corresponds to the predicted value. The presence of P or B would increase the total scattering power for neutron refinements, resulting in an overestimation of the Al content. Site occupancies, refined from the X-ray data, would deviate or decrease only slightly with respect to the theoretical value if B is assigned to the T* site. This seems not to occur, as both X-ray and neutron refinements give results close to the expected values, suggesting that only very limited amounts of P and B, if any, may enter the T* site. An independent assessment is possible by comparing the bond lengths in the T and T* polyhedra. As found also by Angel and Prewitt,[7] the T* site is considerably larger than the tetrahedral site in sillimanite, as would be expected if this site is only 20% occupied. The T site is not completely filled as well; the average T−O bond lengths, however, are shorter than predicted by ionic radius models for a site fully occupied by Al (1.70 vs 1.75 Å),[20] suggesting significant site occupancy by cations with lower ionic radius such as P, as shown in Table 4. In this table the results of 2:1 mullite ($x = 0.4$ in the formula $Al(4 + 2x)Si(2 - 2x)O(10 - x)$) of Angel and Prewitt refer to single-crystal data and are to be compared with sample C, wich derives from 2:1 mullite by substituting Si for 1/2 Al +1/2 B.

For sample G site occupancies of Oc and Oc* were refined on the basis of neutron data. The final results of such refinements are reported in Table 5. The small amount of P in this sample was assigned to the T site, by similarity with the C sample. In the G sample

Table 5. Neutron Atomic Fractional Coordinates and Isotropic Displacement Factors (10^2 Å) of Sample G

	frac occ	x	y	z	U_{iso}
Al (2a)	1.0	0	0	0	1.8(1)
T (4h)	0.495(5) Al	0.149(1)	0.338(1)	0.5	1.8(1)
	0.075 P	0.149(1)	0.338(4)		
T* (4h)	0.221(5) Al	0.269(1)	0.193(1)	0.5	1.8(1)
B (4h)	0.21	0.218(1)	0.284(1)	0.5	1.8(1)
Oab (4g)	1.0	0.3610(2)	0.4166(1)	0.5	2.5(1)
Oc (2d)	0.27(1)	0.5	0	0.5	2.5(1)
Oc* (4h)	0.191(5)	0.454(1)	0.053(1)	0.5	2.5(1)
Od (4h)	1.0	0.1357(2)	0.2129(1)	0	2.5(1)

Table 6. Cell Parameters of the Refined Samples

	a (Å)	b (Å)	c (Å)	V (Å³)
sample C X-ray	7.5767(4)	7.6835(4)	2.8470(1)	165.74(1)
sample C neutron	7.5758(4)	7.6826(3)	1.8458(1)	165.63(1)
sample G X-ray	7.5704(3)	7.6744(3)	2.8393(1)	164.96(1)
sample G neutron	7.5681(4)	7.6691(4)	2.8379(1)	164.71(1)

evidence for B in the triangular site near T was more clearly observed, probably due to the higher B content. B is located almost at the center of a triangle formed by two Od oxygens and an Oab oxygen. Despite different B−O lengths (Table 6), angles of 120(1)° are formed by B with these atoms, confirming the triangular coordination in this sample. It must be stressed, however, that the average bond lengths for this B coordination are longer than for compounds with B in a triangular coordination (1.57 Å vs 1.35−1.38 Å)[21] and moreover the B atom is off-centered within the coordination triangle. This is probably due to fact that the coordinating oxygens are already constrained to their position by a stronger link with other polyhedra. Clearly at the resolution of the X-ray and neutron diffraction it could not be ruled out whether a small amount of residual B could enter tetrahedral sites; X-ray and neutron indipendent refinement however indicated for boron the above structural configuration. Further investigation by NMR analysis would be of interest to detail the issue.The cell parameters of the C and G refinements (X-ray and neutron) are listed in Table 6.

Conclusions

The systematic study of the $Al_2O_3–B_2O_3–P_2O_5$ ternary system allowed us to assess that compositional range $Al_{8+x}P_{1-x}B_{1+x}O_{16+x/2}$ ($0 \le x \le 0.6 \pm 0.1$) corresponds to the pure monophasic mullite-like phase. Structure refinements by indipendent X-ray and neutron diffraction indicate that T* sites are occuped by Al atoms while P and Si are located on T sites. Boron occupies a threefold position, not present in pure Si−Al−O mullite. In this respect the B−P−Al−O mullite behaves differently form BPO_4 silica polymorphic structures, in which boron is tetrahedrally coordinated by oxygen atoms.

(20) Shannon, R. D. *Acta Crystallogr.* **1976**, *A32*, 751.

(21) Jaffe, H. W. *Crystal Chemistry and Refractivity*; Cambridge University Press: Cambridge, U.K.; pp 1−335.